COMPUTER METHODS IN MATERIALS SCIENCE

2023, vol. 23, no. 2, 17–28
https://doi.org/10.7494/cmms.2023.2.0806

Accounting for the random character of nucleation in the modelling of phase transformations in steels

Łukasz Poloczek[1], Roman Kuziak[1], Jakub Foryś[2], Danuta Szeliga[2], Maciej Pietrzyk[2]

[1] Łukasiewicz Research Network, Upper Silesian Institute of Technology, ul. K. Miarki 12, 44-100 Gliwice, Poland.
[2] AGH University of Krakow, al. A. Mickiewicza 30, 30-059 Krakow, Poland.

Abstract

In our earlier work, a stochastic model of multi-stage deformation at elevated temperatures was developed. The model was applied to calculate histograms of dislocation density and grain size at the onset of phase transformation. The histograms were used as input data for the simulation of phase transitions using the traditional deterministic model. Following this approach, microstructural inhomogeneity was predicted for different cooling conditions.

The results obtained, showing the effect of dislocation density and inhomogeneity of austenite grain size on the microstructural inhomogeneity of the final product, can be considered reliable as they are based on material models determined in previous publications and validated experimentally. The aim of the present work was to extend the model by taking into account the stochastic nature of nucleation during phase transitions. The analysis of existing stochastic models of nucleation was performed, and a model for ferritic transformation in steels was proposed. Simulations for constant cooling rates as well as for industrial cooling processes of steel rods were performed. In the latter case, uncertainties in defining the boundary conditions and segregation of elements were also considered. The reduction of the computing costs is an important advantage of the model, which is much faster when compared to full field models with explicit microstructure representation.

Keywords: stochastic model, grain size, phase transformations, dislocation density, cooling of rods, heterogeneity of the microstructure.

1. Introduction

The continuous development of the industry is related to the search for processing routes which allow construction materials with high strength, good formability and a high strength-to-density ratio to be obtained. Steels have met these requirements for many decades. Grain refinement has historically been the primary strengthening mechanism for steels and was studied during the development of high-strength low-alloy steels (HSLA) in the second half of the 20th century (Gladman, 1997). By controlling precipitation and its influence on recrystallization and strengthening, strength and workability were significantly improved (Isasti et al., 2014). Modern multiphase steels which were developed in the last decades of the 20th century employ different strengthening mechanisms. These steels consist of soft ferrite and hard bainite, martensite and islands of retained austenite. The distribution of these constituents is at the macroscopic scale due to the spatial distribution of the volume fractions of the microstructural components.

* Corresponding author: lukasz.poloczek@git.lukasiewicz.gov.pl
ORCID ID's: 0000-0002-0676-9932 (Ł. Poloczek), 0000-0003-4965-5123 (R. Kuziak), 0000-0002-2915-8317 (D. Szeliga), 0000-0002-1473-4625 (M. Pietrzyk)

Advanced numerical models that can predict microstructural heterogeneity are needed to gain insight into the distribution of microstructural features and to design thermomechanical cycles for optimal microstructure and resulting properties. In the work by Szeliga et al. (2019) it was hypothesized that applying stochastic internal variables to the modelling of multiphase steels would allow the construction of models capable of predicting the various characteristics of heterogeneous microstructures.

Although a variety of material models of varying complexity and predictive ability have been developed (Pietrzyk et al., 2015), mean-field models are still widely used for material processing design. The limitations of the current process design methodologies stem from the limited predictive capabilities of these models. This becomes even more important when the prediction of distributions of microstructural parameters rather than average values is required. This is specifically required to improve the impact and fracture toughness of constructional materials. The problem of reliable modelling of heterogeneous microstructure has been solved by full field models, which use RVE (Representative Volume Element) to explicitly represent the microstructure. Applications of the Cellular Automata (Song et al., 2015), the phase-field method (Militzer, 2012) and the FE+LSM (Finite Element + Level Set Method) (Bzowski et al., 2021) have become common during the last two decades. Although these methods can reliably reproduce microstructure evolution, they require long computing times, which is not acceptable when design and optimization of processes are needed. Decreasing computing costs is a crucial task in the present work.

With this motivation in mind, the authors developed a stochastic model describing the evolution of dislocation density and grain size during multi-stage deformation. The analysis and optimization of the numerical parameters of the model is described in (Klimczak et al., 2022), while its detailed description, identification, validation and application in hot rolling is presented in (Szeliga et al., 2022a). The model calculates histograms of dislocation density and grain size after multi-stage deformation. On the other hand, the properties of the final product are maintained by controlling the phase transformation during cooling after deformation. Therefore, our work aimed to extend the model by including the phase transformations during cooling. Accounting for the random character of nucleation of a new phase is the first step towards this objective. The model will also have the capability to account for the uncertainty of the boundary conditions and for the segregation of elements in the banded microstructure.

A literature review shows that stochastic models have been widely used to describe the random nucleation process during phase transformations. However, the majority of the published approaches consider nucleation in the microstructure represented explicitly (full field models). Probabilistic methods have been used in cellular automata models to select nucleation sites or growth directions (Czarnecki et al., 2021; Wang et al., 2014), and in Monte Carlo methods (see Liu et al., 2018) for a review. Rios et al. (2009) consider atomic nuclei located in space in terms of heterogeneous Poisson point processes. They performed computer simulations of point processes in square regions, but the spatial distribution of nucleation probabilities was known a priori. Our objective is to avoid costly computations on the microstructure represented explicitly and to develop a mean-field model based on a statistical description of the phenomena occurring in the microstructure. For steels, the model must be based on the theory of nonclassical nucleation that occurs in diffusional growth, where the diffusion field leads to a decrease in the probability of nucleation around the growth nucleus (Bruna et al., 2006). This aspect is considered in the present work.

Statistical models of nucleation exploiting the "Correlation-Functions" and the "Differential-Critical-Region" were used in (Tomellini & Fanfoni, 2014). It was proved that both methods are suitable for describing phase transformations governed by nucleation and growth. An analysis of these two approaches is presented in (Tomellini & Fanfoni, 2014), with an emphasis on transformations governed by diffusional growth, which cannot be described by the JMAK theory. However, this solution requires numerical calculations of integrals to infinity for many points and is still computationally expensive. Therefore, we focused on the search for a simple model of the probability of nucleation, one based on our knowledge of the physical aspects of nucleation.

The general objective of the research described in this paper was a review of publications on the stochastic models of nucleation and the formulation of the physical and theoretical background for a model which would account for the random character of nucleation of new phases. On the basis of this review, a probability of the nucleation was defined and introduced in the evolution equation. In the first approach, we assumed a stochastic character of the nucleation and a deterministic equation describing the growth of the new phase. Consequently, the opportunity to predict the heterogeneity of the ferrite grain size and phase composition in the final product was created.

2. The general idea of the stochastic phase transformation model

In the model under development, the equilibrium state of the metallurgical system is described by thermodynamics. The phase transformation model predicts changes to the state of the system between the two equilibrium states during the transient process. The equilibrium is represented by the Fe-C phase equilibrium diagram. The following equations obtained from the approximation of the phase boundary lines in this diagram are used as the boundary conditions in the model:

– equilibrium carbon concentration in the austenite (at the γ/α interface):

$$c_{\gamma\alpha} = c_{\gamma\alpha 0} + c_{\gamma\alpha 1} T \tag{1}$$

– maximum carbon concentration in the austenite (at the γ/*cementite* interface):

$$c_{\gamma\beta} = c_{\gamma\beta 0} + c_{\gamma\beta 1} T \tag{2}$$

In Equations (1) and (2) temperature T is in Celsius degrees and $c_{\gamma\alpha 0}$, $c_{\gamma\alpha 1}$, $c_{\gamma\beta 0}$ and $c_{\gamma\beta 1}$ are coefficients, which in our case are determined using ThermoCalc software.

The development of a stochastic phase transformation model for diffusion-controlled transformations is our future objective. The models, which account for the probability of both nucleation and growth, can be encountered in the scientific literature, but they are based on the explicit representation of the microstructure (Lyrio et al., 2019; Rios et al., 2009) and are computationally expensive. Moreover, several published models deal with the solidification process (Maggioni, 2018) or solid-state phase transformations in materials other than steels (Helbert et al., 2004). Thus, in the first approach, we focus on modelling of the random character of the nucleation only and a deterministic model is used to describe the growth of the new phase.

3. Nucleation

3.1. State-of-the-art for nucleation

Nucleation is the first step in all phase transformations occurring in steels. In order to simulate nucleation, it is necessary to specify where the nuclei are located in space and how the nuclei appear as a function of time. In the classical JMAK theory (Johnson–Mehl–Avrami–Kolmogorov) theory (Avrami, 1939; Johnson & Mehl, 1939; Kolmogorov, 1937), there are two main nucleation modes (Liu et al., 2018):

Classical nucleation theory assumes that the thermodynamic properties of the nucleus are homogeneous and identical to their equilibrium volume counterparts within the nucleus, and that the interface between the nucleus and the parent phase is sharp. The nucleation rate depends on the number of critical nuclei, which is determined by the activation energy barrier for heterogeneous nucleation and the jumping frequency of solute atoms across the interface, following the Arrhenius equation.

$$\dot{N}[T(t)] = C\omega \exp\left\{-\frac{\Delta G^*_{het}[T(t)] + Q_N}{RT(t)}\right\} \tag{3}$$

where: $\dot{N}$ – rate of nucleation; C – the density of nucleation sites; ω – the frequency factor; ΔG^*_{het} – the activation energy barrier of heterogeneous nucleation; Q_N – the activation energy of atomic migration across interface; T – temperature; t – time.

Classical nucleation models include: a) sequential nucleation model, b) pre-existing nucleation model, c) Avrami nucleation model and d) hybrid nucleation model. All these models are described in (Liu et al., 2018). The equations describing the nucleation rates of the first three models are given in Table 1, where: N_0 – temperature-independent nucleation rate; N^* – number of nuclei already present per unit volume; δ – Dirac function; φ – cooling rate; λ – frequency at which particles (nuclei) of supercritical size change to particles of subcritical size, following the Arrhenius equation; N' – the number of subcritical particles at $t = 0$.

However, the nucleation process may involve multiple nucleation mechanisms known as hybrid nucleation. The nucleation rate of this model is equal to the weighted sum of the nucleation rates in Table 1.

The non-classical nucleation theory of Cahn and Hilliard is based on the description of interfaces by diffusion (or gradient thermodynamics). In this theory, the coalescence and stepwise nucleation of subcritical clusters are introduced by Ou et al. (2022). Heo et al. (2014) provide a brief overview of recent advances in modelling nucleation during solid-phase transitions based on non-classical descriptions of diffusion interfaces or key nucleation profiles. A method for modelling phase transition dynamics based on differential critical regions and correlation functions is described in the work by Tomellini & Fanfoni (2014). This publication also compares these methods.

Table 1. Equations describing the nucleation rate for different models

Model	Equation	Equation number
1. Continuous nucleation model	$\dot{N}[T(t)] = N_0 \exp\left[-\frac{Q_N}{RT(t)}\right]$	(4)
2. Pre-existing nuclei model	$\dot{N}[T(t)] = N \cdot \delta\left[\frac{T_0 - T(t)}{\varphi}\right]$	(5)
3. Avrami nucleation model	$\dot{N}[T(t)] = \lambda N' \exp\left[-\int_0^t \lambda dt\right]$	(6)

3.2. Stochastic approach to modelling nucleation

From the outset, a stochastic character of nucleation has been accounted for in the modelling of phase transformations, with the JMAK approach based on Poisson statistics being used for many years. Although most of the published papers deal with the crystallization process, solid-state transformations have also been addressed in many publications. Early papers on the stochastic approach to nucleation focused on the study of a random phenomenon such as nucleation by collecting a set of large nucleation data (Izmailov et al., 1999). Izmailov et al. (1999) performed nucleation experiments under the same conditions many times. This approach allowed them to obtain nucleation statistics.

The stochastic models of nucleation have been intensively developed during last few decades. The following assumptions for these models were formulated in the work by Helbert et al. (2004):

- The transformation occurs by nucleation and growth: it is believed that nuclei form at the surface of the parent grain and grow inward. Temperature is only a function of time.
- Nucleation is the process by which atomic nuclei emerge in space and time. Assuming it is a stochastic process, or rather a space-time Poisson process (Stoyan et al., 1987), the average nucleation frequency is expressed as the number of nuclei formed per unit time and per unit surface area (in two dimensions).
- The growth process is deterministic and spatially uniform. For non-isothermal reactions, the radial growth rate γ, is a function of time.

The main stochastic nucleation model is based on a uniform Poisson point process and assumes that the crystallites are randomly distributed in space. This is how the phantom grows at the core of the phantom, sometimes in areas that have been transformed. This leads to a non-randomly occurring phenomenological equation in which the transformation fraction, $X(t)$, at time t is related to the enhanced JMAK volume fraction, X_E, by the relationship:

$$\frac{dX(t)}{dX_E} = [1 - X(t)]^i \tag{7}$$

In the work by Tagami & Tanaka (1997) it is shown that the exponent is expressed as $i = 2 - \xi$, where ξ is the "overlap factor", which accounts for the probability of the overlap between a phantom and a nucleus. This idea of the overgrowth of the phantom nuclei is used in several papers dealing with stochastic modelling of the nucleation.

As already mentioned, no correlation among nuclei is present in the homogeneous Poisson Point Process and, in the case of steels, the probability of a nucleus to appear depends on such parameters as undercooling below A_{e3}, state of the austenite, etc. Thus, assuming Poisson homogenous nucleation and based on the fundamental knowledge regarding nucleation (Clouet, 2009), the probability that the nucleus of the new phase occurs in the time $\Delta t = t_{i+1} - t_i$ is:

$$\mathbf{P}[\xi(t_i) = 0] = \begin{cases} p(t_i) & if \quad p(t_i) < 1 \\ 1 & otherwise \end{cases} \tag{8}$$
$$\mathbf{P}[\xi(t_i) = 1] = 1 - \mathbf{P}[\xi(t_i) = 0]$$

In Equation (8) $p(t_i)$ is a function which bounds together the probability that the material point becomes a critical nucleus in a current time step and present state of material. This probability is based on the following knowledge about nucleation sites: nucleation rate increases with an increase of the undercooling below A_{e3} temperature, grain boundaries and shear bands in the deformed microstructure are the most favourable nucleation sites.

Based on this knowledge, and assuming Poisson homogenous nucleation, the following equation was used:

$$p(t_i) = b_1 D_\gamma^{-b_2} \rho^{b_3} (A_{e3} - T)^{b_4} \quad (9)$$

where: D_γ – grain size; ρ – dislocation density; b_1, b_2, b_3, b_4 – coefficients.

In the numerical solution, in each time step, a random number $s \in [0,1]$ is generated and compared with the probability $p(t_i)$. If the latter is larger, the variable $(t_i) = 0$, and the nucleus of a new phase occurs.

In Equation (9), grain size and dislocation density are stochastic variables, which are calculated by the model described in publication by Szeliga et al. (2022a). Coefficients b_1, b_2, b_3, b_4 can be determined by the inverse analysis of the experimental data (Pietrzyk et al., 2016).

Intensive progress in the development of the stochastic nucleation models has been made in the 21st century. The mathematical background of these models is still based on the statistical methods, which include Poisson point processes. As previously, the transformation kinetics is described by the JMAK equation (Avrami, 1939; Johnson & Mehl, 1939; Kolmogorov, 1937), which is based on Poisson statistics (no correlation among nuclei is present). Rios & Villa (2009) revisited the classical JMAK theory and generalized it for situations in which nucleation took place both for homogeneous and for inhomogeneous Poisson point processes. In the latter intensity of nucleation varies in space. Inhomogeneous Poisson point process nucleation is generally used to account for the heterogeneity of the nucleation sites. In the simulations performed in the work by Rios et al. (2009) nuclei distributed are in space with intensity varying according to a certain function known a priori. Here, X and X_E are replaced by the position-dependent mean bulk density $X(t, x)$, mean extended volume density $X_E(t, x)$, where $x = (x_1, x_2, x_3)$ are the position coordinates. Thus, the relationship between the volume fraction and the expanded volume fraction becomes the relationship between the average bulk density and the average expanded bulk density. The mathematical details of the solution can be found in publication by Rios & Villa (2009).

An example of the solution to this problem assuming site-saturated nucleation and intensity of nucleation distributed linearly along one of the coordinates is presented by Rios et al. (2009). For the Poisson point processer, we obtain:

$$p[N(A) = k] = \frac{\lambda^k(x)}{k!} \exp[-\lambda(x)] \quad (10)$$

where: $p(N(\mathrm{A}) = k)$ – the probability of k nuclei falling within the unit volume A; $\lambda(x)$ – function describing the distribution of the intensity.

In the solution described by Equation (10) the function $\lambda(x)$ has to be known. Our objective is to introduce statistical interaction between existing grains of a new phase and a new nucleus. The solution is based on the critical section approach (Alekseechkin, 2000). Let us find the probability $p(t)$ that a randomly chosen point O transitions to a new phase within the time interval Δt. For this, the following two conditions are sufficient and necessary: a) point O is not transformed before time t_i; b) a new phase nucleus capable of transforming point O within the time interval $[t_i, t_i + \Delta t]$ appears at any time t', $0 < t' < t_i$. By combining the probabilities of the first event and the second event, we obtain a nucleation probability that takes into account the correlation between the nuclei and the existing grains of the new phase:

$$p(t_i) = b_1 D_\gamma^{-b_2} \rho^{b_3} (A_{e3} - T)^{b_4} [1 - X(t_i)] \quad (11)$$

where: $X(t_i)$ – volume fraction of a new phase in the time t_i.

In the case of the austenite decomposition, carbon is pushed out from the ferrite grains and carbon content in the austenite c_γ increases (see next chapter). Thus, the probability of nucleation in the neighbourhood of the new ferrite grains is decreased. This effect can be easily accounted for in the full field model, in which the solution of the carbon diffusion is performed. In our model, we introduced a statistical approach based on the average carbon content in the austenite. The idea of this stochastic approach to modelling austenite-ferrite transformation is shown in Figure 1. Thus, the Equation (11) is revised to the following form:

$$p(t_i) = b_1 D_\gamma^{-b_2} \rho^{b_3} (A_{e3} - T)^{b_4} [1 - X(t_i)] \left(\frac{c_{\gamma\alpha} - c_\gamma}{c_\gamma} \right)^{b_5} \quad (12)$$

where: c_0 – carbon content in steel; c_γ – average carbon content in the austenite, see Equation (17) in the next chapter.

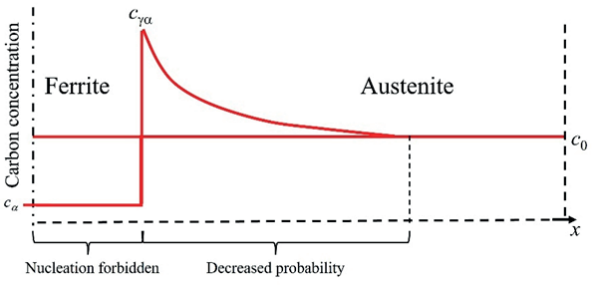

Fig. 1. Carbon distribution as a function of distance from ferrite grain centre and the idea of the stochastic approach to nucleation model based on critical region method

Associated nucleation is also induced in stress-driven switching, where the strain field imparts a degree of spatial ordering to the nuclei (Bruna et al., 2006), but this is not considered in the current work. Recapitulating, we will consider two mechanisms of nucleation in our stochastic model. One is the continuous nucleation model, based on Poisson statistics, in which the nucleation rate is constant at constant temperature (model 1 in Table 1). The other is the non-classical nucleation model, in which growing nuclei of the new phase and carbon diffusion give rise to reduced nucleation probability around this nucleus.

3.3. Modification of the model accounting for the effect of microchemical segregation bands

The solidification process occurs when the dendrites enter the liquid region. As the interface progresses, some solutes are incorporated into the dendrites, while others are released into the fluid. This distribution effect can lead to concentration gradients that lead to microchemical banding (Rivera-Díaz-Del-Castillo et al., 2004). In our model, we will account for the difference in the manganese content between the segregation bands (high Mn, Si, ...) and the distance between the bands (low Mn). Our objective was to include the effect of manganese segregation into the probability of ferrite nucleation defined in Equation (12). The independent variables in the model were the width of the manganese enriched band w and the distance between the bands d. The improved model accounts for a difference in the nucleation rate and the grain size between high and low manganese bands. The driving force for the transformation of austenite to ferrite depends on the Mn concentration and thus varies between microsegregation layers – ferrite tends to form in the Mn-poor bands. On the basis of this knowledge, we proposed the introduction of coefficient b_1 in Equation (12) in a certain interval $[b_{1\min}, b_{1\max}]$ and to revise this equation as follows:

$$p(t_i) = [b_{1\max}(1-\xi) + b_{1\min}\xi] D_\gamma^{-b_2} \rho^{b_3} (A_{e3} - T)^{b_4} \times [1 - X_f(t_i)] \left(\frac{c_{\gamma\alpha} - c_\gamma}{c_\gamma} \right)^{b_5} \quad (13)$$

where: $\xi = w/d$ – relative thickness of the high manganese band.

The $b_{1\min}$ and $b_{1\max}$ coefficients were determined by inverse analysis of the experimental data.

3.4. Growth

As mentioned earlier, the core growth model is deterministic. It is based on an upgrade of the Leblond model (Leblond & Devaux, 1984), which describes the growth kinetics of new phases. The model is based on differential equations with respect to time and does not require the application of additivity rules as the temperature varies in the process. This is the main benefit of this approach. The original Leblond model assumes that the conversion rate is proportional to the distance from thermodynamic equilibrium at a given temperature:

$$\frac{dX(t)}{dt} = B[X_{eq}(T) - X(t)] \quad (14)$$

where: t – time; X – volume fraction of a new phase; X_{eq} – equilibrium volume fraction of the new phase in the temperature T; B – material constant.

In Equation (14) the equilibrium fraction of the new phase in the current temperature is calculated from the equation:

$$X_{eq}(T) = \frac{F_{fT}}{F_{f\max}} = \frac{c_{\gamma\alpha}(T) - c_0}{c_{\gamma\alpha}(T) - c_\alpha} \quad (15)$$

where: F_{fT} – equilibrium volume fraction of the considered phase in steel at the current temperature T; $F_{f\max}$ – maximum volume fraction of this phase in the steel.

The effect of grain size on the phase transition is considered. In addition to temperature, the coefficient B in Equation (14) also depends on the state of the material before the phase transition. In our case, this state can be described by two internal variables: dislocation density and grain size, but only the latter is considered in the present work. The ferrite transformation coefficient B is defined as:

$$B_f = a_6 D^{a_{10}} \exp\left(\frac{|T - a_7|}{a_8} \right)^{a_9} \quad (16)$$

where: D – austenite grain size prior to transformation; a_6, a_7, a_8, a_9, a_{10} – coefficients.

Grain size is a stochastic variable and is calculated using the model developed for hot deformation. The mathematical background of the Monte Carlo solution in this model is described by Klimczak et al. (2022). The formulation of this model for the multistep deformation, as well as identification and validation of the model, are described in publications by Szeliga et al. (2022a, 2022b).

Modelling of phase transformations begins with an Equation (14) when the temperature drops below A_{e3} nucleation of the ferrite occurs. The transformed ferrite volume fraction $X_f(T)$ is calculated with respect to the equilibrium volume fraction of ferrite X_{eut} at the eutectic temperature. Thus, the volume fraction of ferrite with respect to the whole volume of the material is $F_f = X_{eut} X_f$. When the volume fraction of ferrite increases, carbon is pushed out into austenite and the average carbon content in the latter increases following the formula:

$$c_\gamma = \frac{(c_0 - X_f c_\alpha)}{1 - X_f} \tag{17}$$

The simulation continues until the transformed volume fraction reaches 1. However, when the average carbon content in austenite exceeds the limit $c_{\gamma\beta}$ given by Equation (2), the austenite-pearlite transformation starts in the remaining volume of austenite. The kinetics of pearlite transformation is described by Equation (14), where the coefficient B is defined as:

$$B_p = a_{16} D^{a_{20}} \exp\left(\frac{T - a_{17}}{a_{18}}\right)^{a_{19}} \tag{18}$$

where: a_{16}, a_{17}, a_{18}, a_{19}, a_{20} – coefficients.

When the temperature is lower than the bainite transformation start temperature of the state variable a_{20}, the bainite transformation starts. The kinetics of pearlite transformation is described by Equation (14), where the coefficient B has been defined as:

$$B_b = a_{26} D^{a_{30}} \exp\left(\frac{T - a_{27}}{a_{28}}\right)^{a_{29}} \tag{19}$$

where: a_{26}, a_{27}, a_{28}, a_{29}, a_{30} – coefficients.

At temperatures below the martensite initiation temperature, the remaining austenite transforms into martensite. The martensite transformation start temperature is a function of the current average carbon concentration c_γ, in the austenite as follows:

$$M_s = a_{31} - a_{32} c_\gamma \tag{20}$$

where: a_{31}, a_{32} – coefficients.

The volume fraction of the martensite is calculated from the Koistinen and Marburger equation (Koistinen & Marburger, 1959):

$$X_m = 1 - \exp[-a_{33}(M_s - T)^{a_{34}}] \tag{21}$$

where: a_{33}, a_{34} – coefficients.

Equation (21) expresses the volume fraction of martensite relative to the remaining austenite volume at temperature M_s. The volume fraction of martensite relative to the total volume of the material is:

$$F_m = (1 - F_f - F_p - F_b) X_m \tag{22}$$

where: F_f, F_p, F_b – volume fractions of ferrite, pearlite and bainite with respect to the whole volume of the sample.

The model contains several coefficients, which are grouped in the vector $\mathbf{a} = \{a_1, \ldots, a_{32}\}^T$. These coefficients are identified on the basis of dilatometric tests performed for the investigated steel. The inverse approach described by Rauch et al. (2018) was used. The same inverse algorithm was used for the identification of the coefficients $b_1 - b_9$ in the nucleation model and the ferrite grain size model.

The flow of the calculations for the whole model is shown in Figure 2. For each Monte Carlo point, the initial dislocation density is drawn assuming the Gauss distribution with the expected value ρ_0 and the initial grain size is drawn assuming the Weibull distribution with the expected value D_0 (see Szeliga et al., 2022a for details).

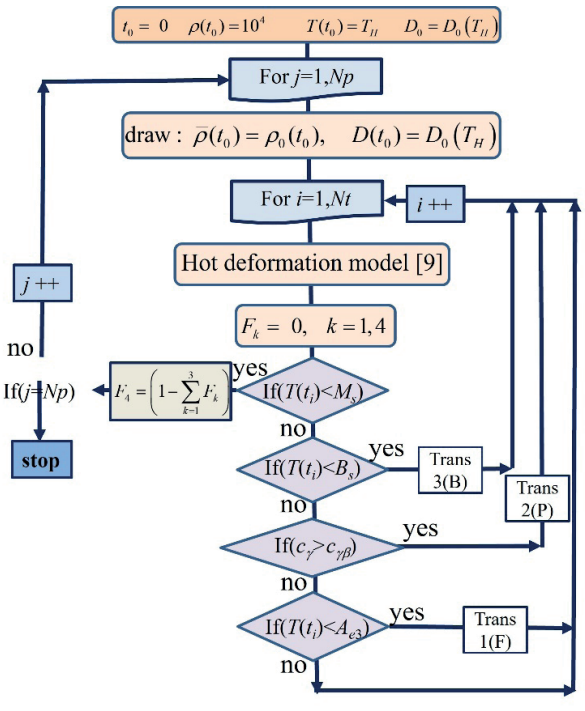

Fig. 2. The flow of the calculations for the whole model composed of the hot deformation and cooling parts: T_H – preheating temperature; t_H – preheating time; D_0 – average grain size after preheating; B_s, M_s – bainite and martensite start temperatures, respectively; c_γ – current carbon concentration in the austenite, $c_{\gamma\beta}$ – equilibrium carbon concentration at the γ-cementite interface, Np – number of the Monte Carlo points, Ns – number of time steps.

Deterministic phase transformation models combine nucleation and growth in one equation, with the JMAK equation being the most often used. Since it is an exponential equation with coefficients dependent on the temperature, it cannot be directly applied to processes in varying temperatures. Therefore, in our model, the growth kinetics of the new phase is described by the ordinary differential Equation (14) based on the Leblond model (Leblond & Devaux, 1984).

3.5. Ferrite grain size

In steels with a carbon equivalent C_{eq} = (C + Mn/6) below about 0.45, ferrite and pearlite transformations occur at low cooling rates. The main parameter of interest here is the ferrite grain size. Ferrite grains have been shown to nucleate at austenite grain boundaries, strain bands, second phase grains and recovered subgrain boundaries, especially when decorated with precipitates. Factors affecting the ferrite grain size are the final austenite grain size (before phase transformation) and residual strain due to incomplete recrystallization, which are external parameters. Retained strain applies to strain that was not removed by recrystallization prior to transformation. Various general relationships for ferrite grain size have been proposed in the literature, some of which are summarized in (Lenard et al., 1999). The deterministic equation proposed by Hodgson & Gibbs (1992) is one of the most commonly used equations in traditional modelling:

$$D_{\alpha} = (1-0.45\varepsilon_r^{1/2})\{(-0.4+6.37C_{eq}) + (24.2-59C_{eq})C_r^{-0.5} + 22[1-\exp(-0.015D_{\gamma})]\} \quad (23)$$

where: ε_r – retained strain, C_{eq} – carbon equivalent, C_r – cooling rate, D_{γ} – austenite grain size prior to transformation [μm].

This equation is suitable for the continuous cooling processes, and it cannot be applied to the isothermal transformations. Therefore, on the basis of the equation (23), in our stochastic model, we proposed a new relationship with the average temperature of transformation as an independent variable. It was assumed that the ferrite grain size depends on the austenite grain size distribution, austenite deformation, average temperature of the ferritic transformation and probability of nucleation:

$$D_f = b_6 \frac{D_{\gamma}^{b_7}}{(A_{e3}-T_{fav})^{b_8}} \rho^{b_9} \quad (24)$$

where: D_{γ} – austenite grain size prior to transformations; ρ – dislocation density; b_6, b_7, b_8, b_9 – coefficients.

In Equation (24) an average temperature of the ferritic transformation is calculated as:

$$T_{fav} = \frac{1}{X_f}\sum_{i=1}^{Nt}(T_i \Delta X_f) \quad (25)$$

where: T_i – temperature in the i-th time step; Nt – number of time steps during ferritic transformation; X_f – final ferrite volume fraction; ΔX_f – increment of the ferrite volume fraction in the i-th time step.

In the present work recrystallization of the austenite was completed before the beginning of the phase transformations and the coefficient $b_9 = 0$ was assumed. After identification of the coefficients b_6, b_7 and b_8, the results obtained from Equations (24) and (23) for constant cooling rates and for $\varepsilon_r = 0$ were similar.

3.6. Numerical tests of the model

In order to evaluate the model's performance, numerical tests were carried out and constant cooling rate experiments were simulated. The austenite grain size prior to transformations was introduced as a histogram, which was measured in the experimental samples after austenitization in the dilatometric tests. The average ferrite grain sizes for the following cooling rates 0.05°C, 0.2°C, 0.5°C, 2°C and 5°C were 10.5 μm, 9.9 μm, 9.3 μm, 8.3 μm, 7.7 μm, respectively. Calculated distributions of the ferrite grain size for different cooling rates are shown in Figure 3. These results confirm the qualitatively good predictive capability of the model. With the increasing cooling rate, the distributions of the ferrite grain size move towards lower values.

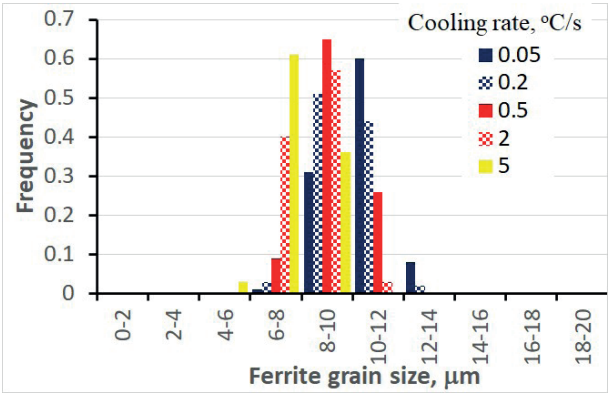

Fig. 3. Calculated distributions of the ferrite grain size for different cooling rates

4. Measurement methodology and research results

4.1. Methodology

Due to the incomplete etching of ferrite grain boundaries (Fig. 4a), in the first stage of the analysis, boundaries corrections were made for better and easier detection (Fig. 4b). In the next step, the ferrite grain size was measured using Met-Ilo v12.1 software. In the first step, *k*-means binarization of the bright phase was carried out. Then, manual corrections were made for elements that were not included or elements that were mistakenly analysed during binarization and also for elements below 3 pixels that were artefacts created in the metallographic process of preparing specimens. The final effect of the detection is shown in Figure 4c.

4.2. Results

The stochastic model predicts distributions (histograms) of parameters such as volume fractions of phases and size of the ferrite grains. A simulation of the cooling of the flat rod with a thickness of 28 mm made from steel containing 0.12% C and 1.3% Mn was performed and the results were compared with the experiment. The measured time-temperature profile, which was used as an input for the phase transformation model, is shown in Figure 5a. Since the difference in the temperatures in the two locations is small, only the results for the centre of the rod are presented below. The time-temperature profiles shown in Figure 5 and the samples after cooling were subject to microstructure analysis. The microstructure after cooling is shown in Figure 5b. The ferrite/pearlite bands are clearly seen in this figure. The measured distance between the high and low manganese bands was 25.8 μm, and it varied in a wide range between 11.2 μm and 39.2 μm.

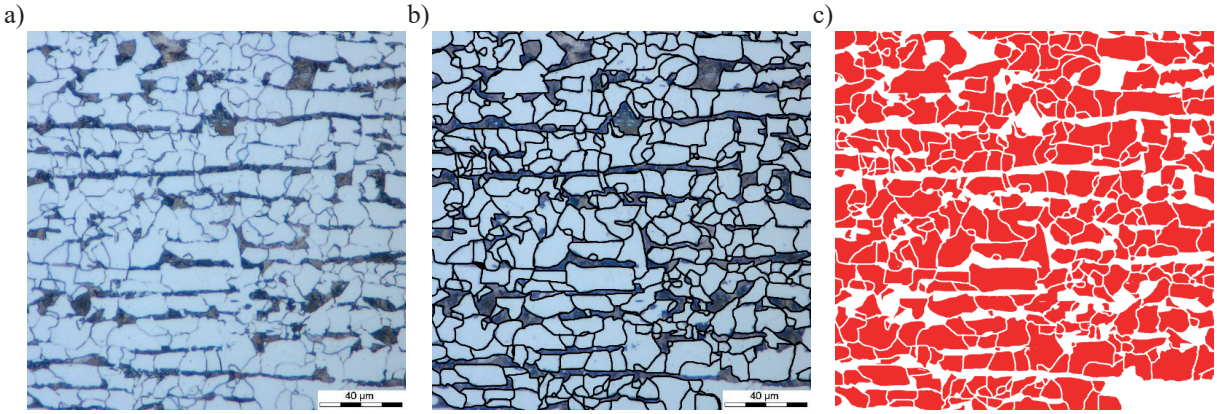

Fig. 4. Ferrite grain size detection procedure: a) output image; b) image after correction of grain boundaries; c) final detection image

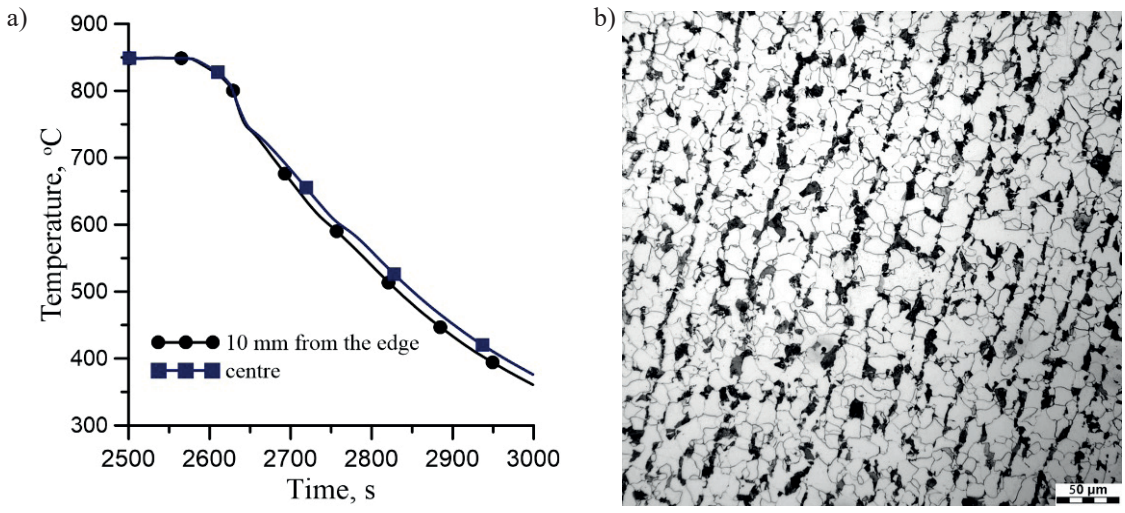

Fig. 5. Measured time-temperature profile during cooling of the 28 mm thick flat rod (a) and microstructure after cooling with ferrite/pearlite bands (b)

In Figure 6, the calculated distribution of ferrite grain size is compared with the measured value. Fairly good agreement was obtained between calculations and measurements. The calculated histogram of ferrite volume fraction after cooling, accounting for the statistical character of the phase transformation, is shown in Figure 6b. The measured average ferrite volume fraction was 0.82.

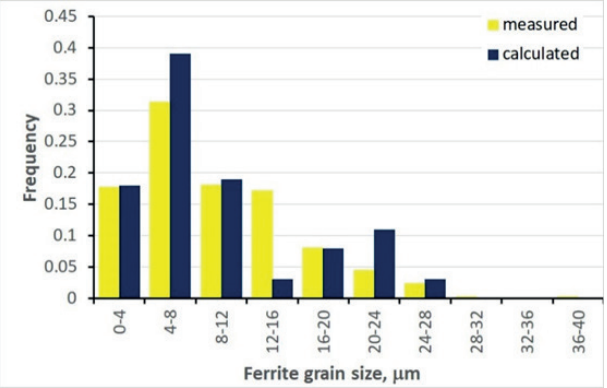

Fig. 6. Comparison of measured and calculated ferrite grain size histograms

The properties of final products depend on the ferrite grain size and the phase composition. The model calculates the stochastic distribution of these parameters, therefore, it can be used to evaluate the uncertainty of the predictions of mechanical properties.

5. Conclusions

A model based on the heterogeneous Poisson point process was proposed for ferritic transformation. Numerical simulations lead to the following conclusions:

- The model belongs to the mean field models, and it does not require an explicit representation of the microstructure. As a consequence of this, computing times could be radically decreased compared to full field models.
- The predictive capabilities were extended compared to the conventional mean field models. The model statistically predicts the distribution of microstructural features instead of their average values. It allows the calculation of distributions (histograms) of selected parameters, taking into account the state of the microstructure before transformation, including the influence of microchemical bands. The uncertainty of the boundary conditions can also be accounted for.
- Since the mechanical properties of final products (strength, elongation) depend on the ferrite grain size and the phase composition, the model can be used to evaluate the uncertainty of the predictions of these properties.

Acknowledgements

The financial assistance of the National Science Foundation in Poland (NCN), project no. 2021/43/B/ST8/01710, is acknowledged.

References

Alekseechkin, N.V. (2000). On calculating volume fractions of competing phases. *Journal of Physics: Condensed Matter*, *12*, 9109–9122. https://doi.org/10.1088/0953-8984/12/43/301.

Avrami, M. (1939). Kinetics of phase change. I. General theory. *Journal of Chemical Physics*, *7*, 1103–1112. https://doi.org/10.1063/1.1750380.

Bruna, P., Crespo, D., González-Cinca, R., & Pineda, E. (2006). On the validity of Avrami formalism in primary crystallization. *Journal of Applied Physics*, *100*, 054907.

Bzowski, K., Rauch, Ł., Pietrzyk, M., Kwiecień, M., & Muszka, K. (2021). Numerical modeling of phase transformations in dual-phase steels using Level Set and SSRVE approaches. *Materials*, *14*(18), 5363. https://doi.org/10.3390/ma14185363.

Czarnecki, M., Sitko, M., & Madej, Ł. (2021). The role of neighborhood density in the random cellular automata model of grain growth. *Computer Methods in Materials Science*, *21*(3), 129–137. https://doi.org/10.7494/cmms.2021.3.0760.

Gladman, T. (1997). *The physical metallurgy of microalloyed steels*. Institute of Materials.

Helbert, C., Touboul, E., Perrin, S., Carraro, L., & Pijolat, M. (2004). Stochastic and deterministic models for nucleation and growth in non-isothermal and/or non-isobaric powder transformations. *Chemical Engineering Science*, *59*(7), 1393–1401. https://doi.org/10.1016/j.ces.2003.12.004.

Heo, T.W., & Chen, L.Q. (2014). Phase-field modeling of nucleation in solid-state phase transformations. *JOM*, *66*, 1520–1528. https://doi.org/10.1007/s11837-014-1033-9.

Hodgson, P.D., & Gibbs, R.K. (1992). A mathematical model to predict the mechanical properties of hot rolled C-Mn and microalloyed steels. *ISIJ International*, *32*(12), 1329–1338. https://doi.org/10.2355/isijinternational.32.1329.

Isasti, N., Jorge-Badiola, D., Taheri, M.L., & Uranga, P. (2014). Microstructural and precipitation characterization in Nb-Mo microalloyed steels: estimation of the contributions to the strength. *Metals and Materials International*, *20*, 807–817. https://doi.org/10.1007/s12540-014-5002-1.

Izmailov, A.F., Myerson, A.S., & Arnold, S. (1999). A statistical understanding of nucleation. *Journal of Crystal Growth*, *196*, 234–242. https://doi.org/10.1016/S0022-0248(98)00830-6.

Johnson, W.A., & Mehl, R.F. (1939). Reaction kinetics in processes of nucleation and growth. *Transactions AIME*, *135*, 416–442.

Klimczak, K., Oprocha, P., Kusiak, J., Szeliga, D., Morkisz, P., Przybyłowicz, P., Czyżewska, N., & Pietrzyk, M. (2022). Inverse problem in stochastic approach to modelling of microstructural parameters in metallic materials during processing. *Mathematical Problems in Engineering*, 9690742. https://doi.org/10.1155/2022/9690742.

Koistinen, D.P., & Marburger, R.E. (1959). A general equation prescribing the extent of the austenite-martensite transformation in pure iron-carbon alloys and plain carbon steels. *Acta Metallurgica*, *7*(1), 59–60. https://doi.org/10.1016/0001-6160(59)90170-1.

Kolmogorov, A. (1937). K statisticheskoy teorii kristallizatsii metallov. *Izvestiya Akademii Nauk SSS. Seriya matematicheskaya*, *1*(3), 355–359 [Колмогоров, А.Н. (1937). К статистической теории кристаллизации металлов. *Известия Академии Наук СССР. Серия математическая*, *1*(3), 355–359].

Lenard, J.G., Pietrzyk, M., & Cser, L. (1999). *Mathematical and Physical Simulation of the Properties of Hot Rolled Products*. Elsevier.

Liu, X., Li, H., & Zhan, M. (2018). A review on the modeling and simulations of solid-state diffusional phase transformations in metals and alloys. *Manufacturing Review*, *5*, 10. https://doi.org/10.1051/mfreview/2018008.

Lyrio, M.S., Alves, A.L.M., Silveira de Sá, G.M., da Silva Ventura, H., da Silva Assis, W.L., & Rios, P.R. (2019). Comparison of transformations with inhomogeneous nucleation and transformations with inhomogeneous growth velocity. *Journal of Materials Research and Technology*, *8*(5), 4682–4686. https://doi.org/10.1016/j.jmrt.2019.08.012.

Maggioni, G.M. (2018). *Modelling and data analysis of stochastic nucleation in crystallization* (Doctoral thesis, ETH Zurich). https://doi.org/10.3929/ethz-b-000250375.

Militzer, M. (2012). Phase field modelling of phase transformations in steels. In: E. Pereloma, & D.V. Edmonds (Eds.), *Phase Transformations in Steels* (Vol. 2: *Diffusionless Transformations, High Strength Steels, Modelling and Advanced Analytical Techniques*, pp. 405–432). Woodhead Publishing.

Ou, X., Sietsma, J., & Santofimia, M.J. (2022). Fundamental study of nonclassical nucleation mechanisms in iron. *Acta Materialia*, *226*, 117655. https://doi.org/10.1016/j.actamat.2022.117655.

Pietrzyk, M., Madej, Ł., Rauch, Ł., & Szeliga, D. (2015). *Computational Materials Engineering: Achieving High Accuracy and Efficiency in Metals Processing Simulations*. Butterworth-Heinemann, Elsevier.

Rauch, Ł., Bachniak, D., Kuziak, R., Kusiak, J., & Pietrzyk, M. (2018). Problem of identification of phase transformation models used in simulations of steels processing. *Journal of Materials Engineering and Performance*, *27*, 5725–5735. https://doi.org/10.1007/s11665-018-3651-9.

Rios, P.R., & Villa, E. (2009). Transformation kinetics for inhomogeneous nucleation. *Acta Materialia*, *57*, 1199–1208.

Rios, P.R., Jardim, D., Assis, W.L.S., Salazar, T.C., & Villa, E. (2009). Inhomogeneous Poisson point process nucleation: comparison of analytical solution with Cellular Automata simulation. *Materials Research*, *12*(2), 219–224. https://doi.org/10.1590/S1516-14392009000200017.

Rivera-Díaz-Del-Castillo, P.E.J., Sietsma, J., & Van Der Zwaag, S. (2004). A model for ferrite/pearlite band formation and prevention in steels. *Metallurgical and Materials Transactions A*, *35*(2), 425–433.

Song, K.J., Wei, Y.H., Dong, Z.B., Wang, X.Y., Zheng, W.J., & Fang, K. (2015). Cellular automaton modeling of diffusion, mixed and interface controlled phase transformation. *Journal of Phase Equilibria and Diffusion*, *36*, 136–148. https://doi.org/10.1007/s11669-015-0369-3.

Stoyan, D., Kendall, W.S., & Mecke, J. (1987). *Stochastic Geometry and Its Applications*. Wiley.

Szeliga, D., Chang, Y., Bleck, W., & Pietrzyk, M. (2019). Evaluation of using distribution functions for mean field modelling of multiphase steels. *Procedia Manufacturing*, *27*, 72–77.

Szeliga, D., Czyżewska, N., Klimczak, K., Kusiak, J., Kuziak, R., Morkisz, P., Oprocha, P., Pietrzyk, M., Poloczek, Ł., & Przybyłowicz, P. (2022a). Stochastic model describing evolution of microstructural parameters during hot rolling of steel plates and strips. *Archives of Mechanical and Civil Engineering*, *22*, 139. https://doi.org/10.1007/s43452-022-00460-2.

Szeliga, D., Czyżewska, N., Klimczak, K., Kusiak, J., Kuziak, R., Morkisz, P., Oprocha, P., Pidvysotsk'yy, V., Pietrzyk, M., & Przybyłowicz, P. (2022b). Formulation, identification and validation of a stochastic internal variables model describing the evolution of metallic materials microstructure during hot forming. *International Journal of Material Forming*, *15*, 53. https://doi.org/10.1007/s12289-022-01701-8.

Tagami, T., & Tanaka, S.-I. (1997). Stochastic modeling of nucleation and growth in a thin layer between two interfaces. *Acta Materialia*, *45*(8), 3341–3347. https://doi.org/10.1016/S1359-6454(97)00021-9.

Tomellini, M., & Fanfoni, M. (2014). Comparative study of approaches based on the differential critical region and correlation functions in modeling phase-transformation kinetics. *Physical Review E*, *90*, 052406. https://doi.org/10.1103/PhysRevE.90.052406.

Wang, Z.-J., Luo, S., Song, H.-W., Deng, W.-D., & Li W.-Y. (2014). Simulation of microstructure during laser rapid forming solidification based on cellular automaton. *Mathematical Problems in Engineering*, 627528. https://doi.org/10.1155/2014/627528.